



**Providing Choice & Value**  
Generic CT and MRI Contrast Agents

**FRESENIUS  
KABI**

**CONTACT REP**

# AJNR

## **Are Linear Measurements of the Nucleus Basalis of Meynert Suitable as a Diagnostic Biomarker in Mild Cognitive Impairment and Alzheimer Disease?**

K.D. Jethwa, P. Dhillon, D. Meng, D.P. Auer and for the Alzheimer's Disease Neuroimaging Initiative

This information is current as of July 29, 2025.

*AJNR Am J Neuroradiol* 2019, 40 (12) 2039-2044

doi: <https://doi.org/10.3174/ajnr.A6313>

<http://www.ajnr.org/content/40/12/2039>

# Are Linear Measurements of the Nucleus Basalis of Meynert Suitable as a Diagnostic Biomarker in Mild Cognitive Impairment and Alzheimer Disease?

 K.D. Jethwa,  P. Dhillon,  D. Meng, and  D.P. Auer,  
for the Alzheimer's Disease Neuroimaging Initiative

## ABSTRACT

**BACKGROUND AND PURPOSE:** Cell loss within the nucleus basalis of Meynert is an early event in Alzheimer disease. The thickness of the nucleus basalis of Meynert (NBM) can be measured on structural MR imaging. We investigated NBM thickness in relation to cognitive state and biochemical markers.

**MATERIALS AND METHODS:** Mean bilateral nucleus basalis of Meynert thickness was measured on coronal T1-weighted MR imaging scans from the Alzheimer's Disease Neuroimaging Initiative dataset. Three hundred and fifteen scans (80 controls, 79 cases of early mild cognitive impairment, 77 cases of late mild cognitive impairment and 79 cases of Alzheimer disease) were assessed. Alzheimer's Disease Assessment Scale-Cognitive scores, CSF tau, and amyloid quantification were extracted. Group differences in NBM thickness, their correlates and measurement reliability were assessed.

**RESULTS:** Mean NBM thickness  $\pm$  SD progressively declined from  $2.9 \pm 0.3$ ,  $2.5 \pm 0.3$ , and  $2.3 \pm 0.3$  to  $1.8 \pm 0.4$  mm in healthy controls, patients with early mild cognitive impairment, late mild cognitive impairment and Alzheimer disease respectively ( $P < .001$ ). NBM thickness was negatively correlated with Alzheimer's Disease Assessment Scale-Cognitive scores ( $r = -0.53$ ,  $P < .001$ ) and weakly positively correlated with CSF amyloid ( $r = 0.250$ ,  $P < .001$ ) respectively. No association with CSF tau was found. NBM thickness showed excellent diagnostic accuracy to differentiate Alzheimer disease (area under the curve, 0.986) and late mild cognitive impairment from controls (area under the curve, 0.936) with excellent sensitivity, but lower specificity 66.7%. Intra- and inter-rater reliability for measurements was 0.66 and 0.47 ( $P < .001$ ).

**CONCLUSIONS:** There is progressive NBM thinning across the aging-dementia spectrum, which correlates with cognitive decline and CSF markers of amyloid- $\beta$  pathology. We show high diagnostic accuracy but limited reliability, representing an area for future improvement. NBM thickness is a promising, readily available MR imaging biomarker of Alzheimer disease warranting diagnostic-accuracy testing in clinical practice.

**ABBREVIATIONS:** A $\beta$  = amyloid  $\beta$ ; AD = Alzheimer disease; ADAS-cog = Alzheimer's Disease Assessment Scale-Cognitive; ADNI = Alzheimer's Disease Neuroimaging Initiative; EMCI = early mild cognitive impairment; LMCI = late mild cognitive impairment; MCI = mild cognitive impairment; NBM = nucleus basalis of Meynert; P-tau = phospho-tau

Alzheimer disease (AD) is a common neuropsychiatric disorder characterized by progressive cognitive impairment, behavioral disturbance, and functional decline. There are currently

around 850,000 individuals living with the disorder in the United Kingdom, and this number is set to rise with an aging population.<sup>1</sup> Impaired quality of life and increased caregiver burden are associated with health service use and associated costs.

There has been much research interest into the pathologic mechanisms that underlie the disorder.<sup>2</sup> The presence of extracellular aggregates (or "plaques") of misfolded amyloid- $\beta$  protein

Received May 30, 2019; accepted after revision September 3.

From the Department of Radiological Sciences, Division of Clinical Neuroscience, School of Medicine; Sir Peter Mansfield Imaging Centre, School of Medicine; and National Institute for Health Research Nottingham Biomedical Research Centre (K.D.J., P.D., D.M., D.P.A.), Queen's Medical Centre, University of Nottingham, Nottingham, UK.

Data used in preparation of this article were obtained from the Alzheimer's Disease Neuroimaging Initiative data base (adni.loni.usc.edu). Thus, the investigators within the Alzheimer's Disease Neuroimaging Initiative contributed to the design and implementation of Alzheimer's Disease Neuroimaging Initiative and/or provided data but did not participate in analysis or writing of this report. A complete listing of Alzheimer's Disease Neuroimaging Initiative investigators can be found at: [http://adni.loni.usc.edu/wp-content/uploads/how\\_to\\_apply/ADNI\\_Acknowledgement\\_List.pdf](http://adni.loni.usc.edu/wp-content/uploads/how_to_apply/ADNI_Acknowledgement_List.pdf).

K.D.J. and P.D. are supported by a National Institute of Health Research Academic Clinical Fellowship in Radiology.

Part of this work was previously presented as a poster at: European Congress of Neuropsychopharmacology, March 8–10, 2018; Nice, France.

Please address correspondence to K.D. Jethwa, FRCR, Radiological Sciences, University of Nottingham, Queens Medical Centre, Derby Rd, Nottingham, NG7 2UH UK; e-mail: [ketan.jethwa@nottingham.ac.uk](mailto:ketan.jethwa@nottingham.ac.uk)  
<http://dx.doi.org/10.3174/ajnr.A6313>

and intracellular “tangles” of hyperphosphorylated tau protein are the pathologic hallmarks of the disease.<sup>3</sup> The presence of these plaques and tangles results in neuroinflammation, neurodegeneration, and subsequent cognitive impairment.<sup>2</sup> Abnormal amyloid- $\beta$  accumulates principally within neocortical areas, while tau is found mainly within the basal forebrain and limbic regions before involving the neocortex, spreading via corticocortical axonal projections. The burden of tau pathology is mostly correlated with the degree of neurodegeneration and cognitive impairment observed clinically.<sup>4</sup>

The nucleus basalis of Meynert (NBM) consists of a population of hyperchromic, magnocellular neurons within the basal forebrain, which represent the main source of cortical cholinergic innervation.<sup>5</sup> The internal structure of the nucleus basalis of Meynert is complex, lacking strict anatomic boundaries, with differentially located neurons projecting to distinct areas of the allocortex and neocortex.<sup>6</sup>

Neurons within the NBM are particularly susceptible to tau pathology, being affected more severely and at an earlier stage of the disease.<sup>5,6</sup> There is a long latent period during which there is increasing tau deposition and cell damage, which precedes cell death and the emergence of clinical symptoms. This latent period may coincide with the presymptomatic and mild cognitive impairment (MCI) phases of AD. Atrophy of temporal lobe structures, including the hippocampal formation and entorhinal cortex, is observed later in the course of AD.<sup>7,8</sup>

Stepwise reductions in NBM volumes have been documented as subjects progress from cognitively normal to MCI and AD.<sup>9</sup> NBM atrophy may also predict MCI-to-AD conversion.<sup>10,11</sup> NBM atrophy may identify patients with late-life depression who are at an increased risk of developing dementia, probably due to a basal forebrain cholinergic deficit.<sup>12</sup> NBM atrophy also appears to be associated with treatment response to cholinesterase inhibitors.<sup>13,14</sup> However, this effect may diminish as NBM atrophy progresses in later stages of the disease.<sup>15</sup> MR imaging functional connectivity analyses have also demonstrated reduced NBM-cortical connectivity in dementia, which may also be of value in predicting treatment response.<sup>16</sup>

The NBM can be readily identified on structural neuroimaging, and its thickness can be measured. NBM thickness measurement is a potentially practical tool, which could be easily used by clinicians to assess subtle pathologic changes in patients with cognitive impairment. There is currently a knowledge gap in terms of whether simple measurements of the basal cholinergic nuclei are altered across the aging-dementia spectrum and whether they are correlated with clinical and biochemical markers of disease.

In this study, we investigated the potential of NBM thickness measurements as a diagnostic marker of Alzheimer disease. We analyzed a well-characterized cohort of 315 subjects from the Alzheimer's Disease Neuroimaging Initiative data base (ADNI; [adni.loni.usc.edu](http://adni.loni.usc.edu)) across the aging-dementia spectrum to test the following hypotheses: that NBM thickness 1) progressively decreases in cognitively healthy elderly subjects during early and late MCI to AD, 2) correlates positively with cognitive performance and negatively with CSF disease markers (phospho-tau [P-tau] and amyloid load), and 3) has potential as clinical

diagnostic marker based on diagnostic accuracy and reliability assessment.

## MATERIALS AND METHODS

### Study Participants

Data used in the preparation of this article were obtained from the ADNI data base. ADNI was launched in 2003 as a public-private partnership. The primary goal of ADNI is to test whether serial MR imaging, PET, other biologic markers, and clinical and neuropsychological assessments can be combined to measure the progression of MCI and early AD. Written informed consent was obtained from all individuals.

A retrospective cohort study was performed using 315 coronally acquired T1-weighted MPRAGE scans from this dataset. Cases were selected consecutively from the dataset. Imaging was acquired on 3T systems across multiple sites and providers with the same ADNI 3T imaging protocol. The sample included 80 healthy controls, 79 individuals with early MCI, 77 with late MCI, and 79 with AD (diagnostic criteria: <https://adni.loni.usc.edu/wp-content/uploads/2008/07/adni2-procedures-manual.pdf>). All patients were 55–90 years of age (inclusive). Sex and years of education were also extracted. Clinical cognitive assessments included the Mini-Mental State Examination and Alzheimer Disease Assessment Scale-Cognitive subscale (ADAS-Cog). Stable dose cholinesterase inhibitors were permitted for patients with MCI and AD (ie, no dose change during the preceding 12 weeks).

### CSF Amyloid and Tau Pathology

We manually extracted the presence of CSF amyloid- $\beta$  (A $\beta$ ) 42 and P-tau from <http://www.ADN.org>. The details of how we extracted the information have been documented previously.<sup>16</sup> The cutoffs for abnormal CSF amyloid  $\beta$ -42 used in this study have been reported previously and were as follows: normal CSF amyloid- $\beta$ -42 (participants with negative CSF A $\beta$ -42 status), >201.6 ng/L and abnormal amyloid- $\beta$  42 (participants with positive CSF A $\beta$ -42 status), <182.4 ng/L.<sup>17</sup> We also used the cutoffs for abnormal P-tau as follows: P-tau-positive ( $\geq$ 23 pg/mL) and P-tau-negative (<23 pg/mL). There is some overlap between normality and disease states (MCI/AD) for these cutoffs. Detailed protocols for the ADNI2 cohort can be found on-line at: <http://adni.loni.usc.edu/adni-go-adni-2-clinical-data-available/>.

### Measurement of NBM Thickness

Images were analyzed using ITK-SNAP software ([www.itksnap.org](http://www.itksnap.org)).<sup>18</sup> A vertical line was drawn from the ventral pallidum to the base of the brain at the section where the anterior commissure crosses the midline. NBM thickness (in millimeters) was measured bilaterally, and a mean NBM thickness was calculated for each case. *Figs 1 and 2* demonstrate the anatomic localization of the NBM on MR imaging.

A second rater (P.D., with 3 years of experience) measured the NBM thickness on both hemispheres independently in 40 participants (10 from each clinical group) following the same method as the first rater (K.D.J., with 3 years of experience) to test the interrater reliability. The intrarater measurements were undertaken by the same assessor with a 4-week interval.

## Statistical Analysis

All statistical analyses were conducted in SPSS (Version 24; IBM, Armonk, New York). One-way ANOVA and  $\chi^2$  tests were used to compare demographics, CSF amyloid pathology, CSF tau pathology, and *apolipoprotein E 4* (APOE 4) status among healthy controls and those with early mild cognitive impairment (EMCI), late mild cognitive impairment (LMCI), and AD.

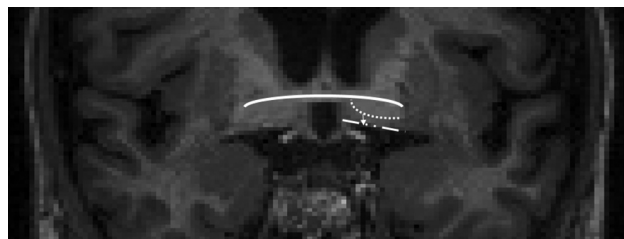


**FIG 1.** Representative coronal MPRAGE brain image showing the localization of the NBM and thickness measurement (arrow). The NBM was measured at its midpoint at the level of the decussation of the anterior commissure (solid line). The NBM sits between the chiasmatic cistern inferiorly (line-dot) and the ventral pallidum superiorly (dotted line). Contrast was maximized on individual cases to improve visualization.

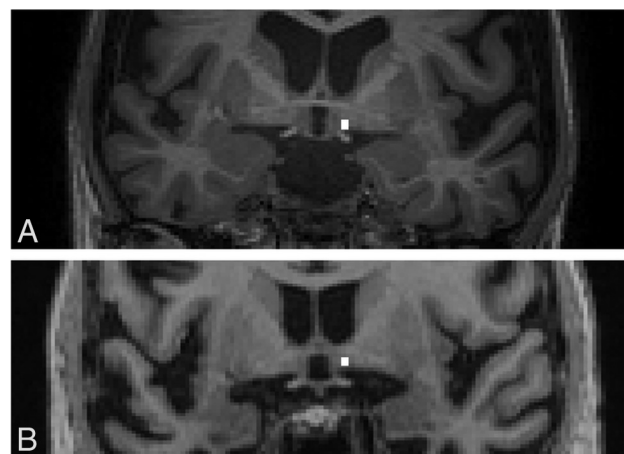


**FIG 2.** Representative coronal MPRAGE brain images showing the localization of the NBM and thickness measurement (white line). A, A patient with AD shows reduced NBM thickness. B, Control. Measurements were made using the ITK-SNAP software.

Due to the between-group differences in age, we then assessed whether NBM thickness was affected by age or sex in our study sample and also explored laterality effects to assess the appropriateness of averaging.

To test our first hypothesis that the averaged NBM thickness was significantly different across healthy controls, EMCI, LMCI, and AD, we used 1-way ANOVA. Data are given as mean  $\pm$  SD unless stated otherwise. Significance was set at  $P < .05$ .

To test our second hypothesis that NBM thickness was declining with increasing cognitive decline and increasing biochemical disease load, we used univariate linear regression analysis to investigate the correlation between averaged NBM thickness and the ADAS-cog score, CSF amyloid- $\beta$  pathology, and CSF tau load. The significance level was set at  $P < .05$ .

To test our third hypothesis that NBM thickness has diagnostic biomarker potential, we used receiver operating characteristic analysis. The choice of the most suitable NBM thickness cutoff to diagnose AD and those at risk based on the Youden index (J) which the maximum value of the index may be used as a criterion for selecting the optimum cutoff point.<sup>19</sup> J can be formally defined as  $J = \text{Sensitivity} + \text{Specificity} - 1$ . We analyzed 2 classification tasks: AD versus controls and LMCI versus controls. We split the sample into 50 controls and 50 cases of AD/LMCI, respectively, to determine the best cutoff and used the remaining 30 controls versus 29 cases of AD and 27 of LMCI, respectively, for validation. We report sensitivity and specificity.

Lastly, using the average value of NBM thickness of the left and right hemispheres, intraclass correlation coefficients were calculated as a measure of interrater (2-way random effects, absolute consistency) and intrarater reliability (mixed-effects model) between 2 radiology trainees to explore the feasibility of clinical implementation. Intraclass correlation coefficient  $> 0.75$  represents excellent reliability; 0.60–0.74, good reliability; 0.41–0.59, fair reliability; and  $< 0.40$ , poor reliability.<sup>20</sup>

## RESULTS

A total of 315 participants (mean age,  $73.2 \pm 7.4$  years; 145 women [46%] and 170 men [54%]) were included. Age ( $P < .001$ ), years of education ( $P = .022$ ), and ADAS-cog scores ( $P < .001$ ) were significantly different among healthy controls and those with EMCI, LMCI, and AD (Table).

### Demographics and clinical information

Whole Sample	Healthy Controls (n = 80)	EMCI (n = 79)	LMCI (n = 77)	AD (n = 79)	P
Age (mean) (yr)	$75.2 \pm 6.4$	$70.2 \pm 7.7$	$72.3 \pm 7.2$	$75.0 \pm 7.5$	$< .001^a$
Female (No.) (%)	41 (51.3)	36 (45.6)	32 (41.6)	36 (45.6)	.680
Education (mean) (yr)	$16.4 \pm 2.3$	$15.9 \pm 2.7$	$16.5 \pm 2.7$	$15.3 \pm 3.1$	.022 <sup>a</sup>
ADAS-cog score (mean)	$9.7 \pm 4.3$	$11.9 \pm 5.4$	$18.3 \pm 6.2$	$30.4 \pm 6.9$	$< .001^a$
CSF amyloid subsample (n = 53)		(n = 68)	(n = 54)	(n = 47)	
CSF A $\beta$ -42 (ng/L) (mean)	$192.5 \pm 56.3$	$193.5 \pm 50$	$166.6 \pm 52.3$	$137.4 \pm 32$	$< .001^a$
Positive CSF A $\beta$ -42 status (No.) (%)	26 (49.1)	25 (36.8)	36 (66.7)	45 (95.7)	$< .001^a$
CSF tau subsample (n = 31)		(n = 68)	(n = 48)	(n = 20)	
CSF P-tau (pg/mL) (mean)	$38.9 \pm 28.8$	$35.1 \pm 21.7$	$44.1 \pm 21.0$	$58.1 \pm 26.2$	.002 <sup>a</sup>
Positive CSF P-tau status (No.) (%)	22 (71.0)	42 (61.8)	41 (85.4)	19 (95.0)	.004 <sup>a</sup>
APOE subsample (n = 78)		(n = 75)	(n = 74)	(n = 77)	
APOE-4 carriers (No.) (%)	25 (32.1)	31 (41.3)	37 (50.0)	50 (64.9)	$< .001^a$

<sup>a</sup> Significant.

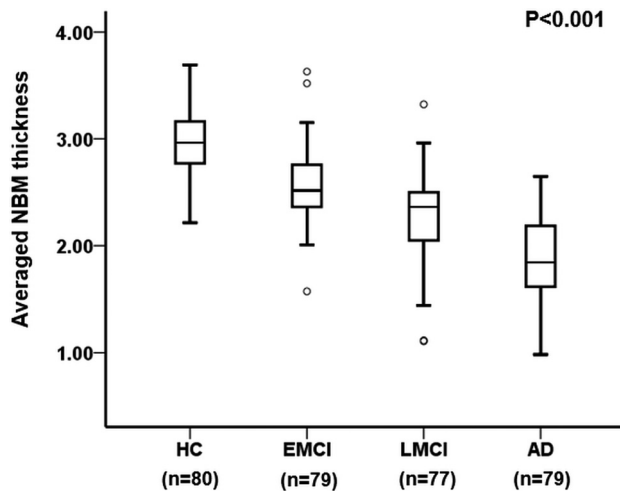


**FIG 3.** Boxplot showing averaged NBM thickness across healthy controls ( $n=80$ ) and individuals with mild cognitive impairment, considered to be early ( $n=79$ ); those with late mild cognitive impairment ( $n=77$ ); and those with AD ( $n=79$ ). NBM thickness differed significantly across cognitive subgroups ( $P < .001$ ).

These significant differences of age ( $P = .006$ ), years of education ( $P = .042$ ), and ADAS-cog scores ( $P < .001$ ) among healthy controls and those with EMCI, LMCI, and AD were also observed in the subsample of participants who had CSF  $A\beta$ -42 measurements ( $n=222$ ). However, in the subsample of participants who had the measurement of CSF P-tau ( $n=167$ ), only the ADAS-cog score ( $P < .001$ ) was significantly different among healthy controls and those with EMCI, LMCI, and AD.

NBM thickness was not significantly affected by age or sex or laterality. Hence, we averaged right and left metrics and did not control for demographic variables. There were statistically significant differences among cognitive subgroup means: healthy controls,  $2.9 \pm 0.3$  mm; early MCI,  $2.5 \pm 0.3$  mm; late MCI,  $2.3 \pm 0.3$  mm; clinical AD,  $1.8 \pm 0.4$  mm as determined by 1-way ANOVA ( $F[3,311] = 128.5$ ,  $P < .001$ ) (Fig 3).

NBM thickness was significantly correlated with cognitive performance with higher ADAS-cog scores found in subjects with thinner NBMs, explaining 33% of the mutual variance ( $r^2 = 0.334$ ,  $P < .001$ , Fig 4). There was also a mild association between a thinner NBM and lower CSF  $A\beta$ -42 ( $r^2 = 0.06$ ,  $P < .001$ , Fig 5). Conversely, CSF P-tau did not correlate with NBM thickness.

The receiver operating characteristic showed excellent diagnostic accuracy to differentiate healthy controls from those with AD (area under the curve, 0.986;  $P < .001$ ; 95% CI, 0.969–1.000; Fig 6A) in the discovery dataset (sensitivity, 92%; specificity, 100%), using a cutoff score of 2.7025 mm. Applying this cutoff to the validation data of 30 controls and 29 patients with AD, we achieved 100% sensitivity but only 66.7% specificity. Considerable overlap of error bars in boxplots among different groups (Fig 3) may account for this specificity value.

Diagnostic accuracy was also excellent to differentiate those with LMCI and controls using the receiver operating characteristic in the discovery subgroup that identified a cutoff of 2.687 mm (area under the curve, 0.936;  $P < .001$ ; 95% CI, 0.884–0.988; Fig 6B) with a sensitivity of 92% and specificity of 90%. Validation in

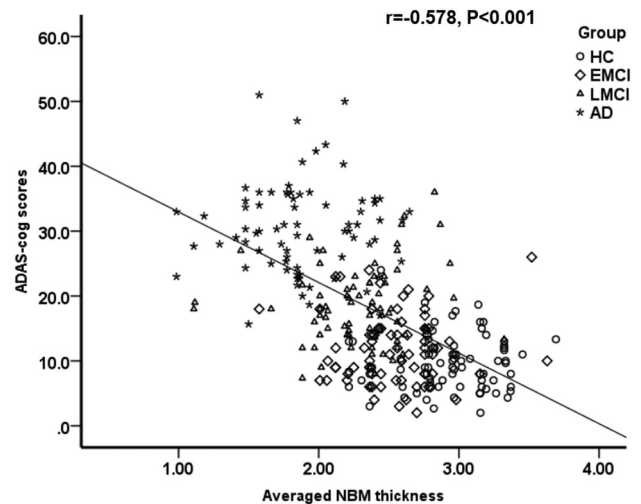


**FIG 4.** Scatterplot shows a negative correlation between cognitive performance (ADAS-cog score) and averaged NBM thickness (in millimeters).

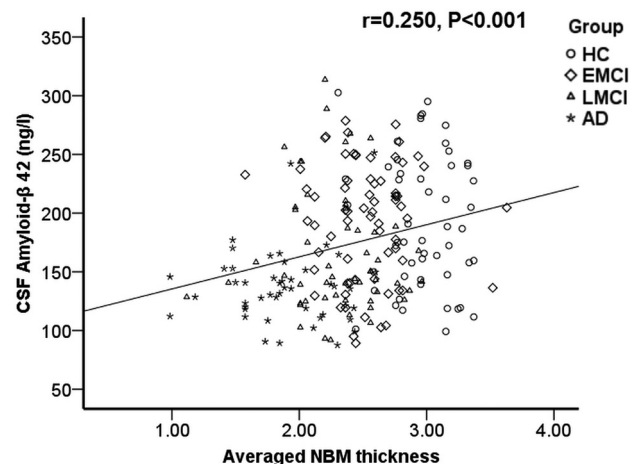


**FIG 5.** Scatterplot shows a positive correlation between CSF  $A\beta$ -42 and averaged NBM thickness.

the remainder of healthy controls and the LMCI cohort (30 healthy controls versus 27 with LMCI) achieved excellent sensitivity (92.5%), at a lower specificity of 66.7%.

A sample of 40 scans was reviewed twice by the same assessor following a 4-week interval to assess intratester reliability. The interrater reliability was considered fair (intraclass correlation coefficient [2,2] = 0.468 [95% CI, -0.227–0.774],  $P < .001$ ), and the intratester reliability was good (intraclass correlation coefficient [2,2] = 0.658 [95% CI, 0.266–0.831],  $P < .001$ ).

## DISCUSSION

In this large retrospective study of a well-phenotyped cohort from the ADNI data base, we undertook a series of qualification studies to assess the potential of a simplified NBM thickness measurement as a novel diagnostic biomarker of AD. We demonstrate progressive thinning of the NBM in subjects with early and late MCI and AD compared with cognitively healthy



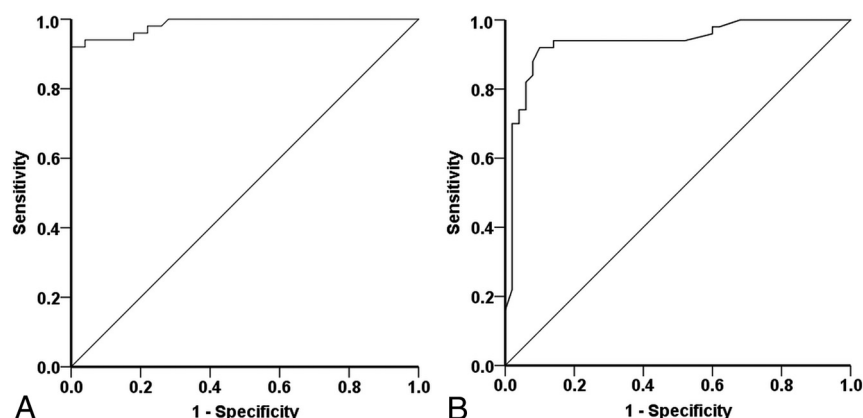


**FIG 6.** Receiver operating characteristic curves to differentiate those with AD from controls (A) and those with LMCI from controls (B).

subjects. Second, we show that linear NBM thickness measures are correlated with measures of cognitive impairment and CSF-A $\beta$ . Lastly, NBM thickness proved promising to differentiate those with AD and late MCI from cognitively healthy controls.

NBM thinning in AD has face validity as a diagnostic marker of AD based on the established cell loss within the NBM in AD, which is well-documented in the pathologic<sup>6</sup> and clinical imaging literature.<sup>9,10</sup> Our findings, using a simple linear assessment of the width of the NBM, closely mirror the reported progressive NBM volumetric reductions in clinical groups with increasing clinical cognitive impairment.<sup>9</sup> Accurate volumetric assessment of the NBM, however, does not form part of routine assessment, and the software required is not available on reporting workstations. Given that the NBM can be readily identified on coronal MR imaging, thickness measurement at the level of the decussation of the anterior commissure may represent a novel and simple-to-use imaging biomarker for routine assessment in memory clinics with no additional scan or software license costs. Small observational studies have previously highlighted differences in NBM thickness between controls and patients with AD and reported mean NBM thicknesses of up to 3.0 mm in controls and 2.1 mm in those with AD.<sup>21</sup> These reports are quantitatively consistent with our findings of 2.9 and 1.8 mm in controls and patients with AD, respectively.

To further qualify MR imaging-defined NBM thickness assessment as a potential biomarker of AD, we sought to address the requirement of a direct association with clinical symptoms and biochemical disease markers. As an important proof of concept, we demonstrated that NBM thinning was significantly correlated with cognitive decline. We found a moderate negative correlation between NBM thickness and ADAS-cog scores, explaining a third of the mutual variance, which corroborates the expected direct role of cholinergic projections from the NBM and cognitive functioning. Preclinical studies have shown memory impairment and learning deficits after lesioning of the NBM.<sup>22</sup> A previous MR imaging study found a significant-albeit-weaker ( $r^2 = 0.12$ ) correlation between the volume of the substantia innominata and memory scores in a cohort of healthy elderly and those with amnesic MCI and AD.<sup>23</sup>

CSF A $\beta$ -42 is an accepted biomarker of cerebral amyloid accumulation, with high diagnostic accuracy for AD.<sup>24</sup> In a subset of the ADNI cohort with available CSF A $\beta$ -42 data, we show that reduced A $\beta$ -42 was associated with reduced NBM thickness, which is consistent with a link between cerebral amyloid pathology and NBM degeneration in AD. There is evidence that NBM atrophy may correlate more closely with cortical amyloid burden than hippocampal atrophy and may predict disease trajectory.<sup>11,25</sup>

The burden of tau pathology is mostly correlated with the degree of clinical cognitive impairment.<sup>4</sup> Hyperphosphorylated tau is preferentially deposited within the basal forebrain early in the course of AD. However, no significant association between CSF P-tau and NBM thickness was identified. A possible explanation is that given that tau is an intracellular protein, there may be limited correlation between CSF levels and the actual cortical burden. A CSF-pathologic correlative study has found no correlation between CSF P-tau levels and the Braak staging criteria, which are used to pathologically assess the burden of cellular tau deposition.<sup>26</sup>

NBM thickness measurement sensitivity and specificity compare favorably with those of currently used structural brain rating scales, including the medial temporal lobe atrophy scale (85% and 82% sensitivity and specificity, respectively).<sup>27</sup> A 2.7-mm cutoff provides superior sensitivity and specificity for distinguishing controls and those with AD as well as controls and those with LMCI in our discovery data, with high sensitivity in the validation data pointing to the potential clinical diagnostic value of NBM thickness as screening biomarker for AD.

The cross-sectional nature of this project and lack of out-of-sample validation are a limitation of this study. Longitudinal analysis is warranted to assess the trajectory of NBM thickness and the power to differentiate stable MCI from MCI-to-AD converters. Second, NBM atrophy measurements are indirect markers of cellular damage and may also reflect changes in other neuronal or glial components within the basal forebrain. Without a postmortem sample, the relationship between NBM thickness and cell count remains unclear. Suboptimal measurement reliability is another limitation of this study. There is fair intrarater and good interobserver reliability for repeat NBM thickness measurements. It is possible that this may be improved with additional rater training and optimizing sequences with better contrast resolution between the NBM and surrounding structures.<sup>28</sup>

## CONCLUSIONS

There is progressive nucleus basalis of Meynert thinning across the aging-dementia spectrum, which correlates with cognitive decline and CSF markers of amyloid- $\beta$  pathology. We show high diagnostic accuracy but limited reliability measurement, which

could be improved by optimising contrast resolution at the base of the brain. Nucleus basalis of Meynert thickness is a promising, readily available MR imaging biomarker of Alzheimer disease which warrants diagnostic-accuracy testing in clinical practice.

Disclosures: Ketan D. Jethwa—UNRELATED: Employment: National Institute of Health Research, Comments: K.D.J. and P.D. are National Institute of Health Research academic clinical fellows whose salary is partly funded by the National Institute of Health Research. This fellowship also includes a bursary for research/educational purposes. Dorothee P. Auer—UNRELATED: Grants/Grants Pending: National Institute of Health Research, Parkinson's UK, Versus Arthritis, Michael J Fox Foundation, Comments: grant funding for unrelated work\*; Other: Biogen, Comments: research support for neuromelanin imaging in Parkinson disease. \*Money paid to the institution.

## REFERENCES

1. What is dementia? Factsheet 400LP January 2017. [https://www.alzheimers.org.uk/Download/Downloads/Id/3416/What\\_Is\\_Dementia.pdf](https://www.alzheimers.org.uk/Download/Downloads/Id/3416/What_Is_Dementia.pdf). Accessed May 3, 2017
2. Esiri MM, Morris JH. *The Neuropathology of Dementia*. Cambridge: Cambridge University Press; 2009
3. Selkoe DJ. Alzheimer's disease: genes, proteins, and therapy. *Physiol Rev* 2001;81:741–66 [CrossRef Medline](#)
4. Braak H, Alafuzoff I, Arzberger T, et al. Staging of Alzheimer disease-associated neurofibrillary pathology using paraffin sections and immunocytochemistry. *Acta Neuropathol* 2006;112:389–404 [CrossRef Medline](#)
5. Mesulam MM. Cholinergic circuitry of the human nucleus basalis and its fate in Alzheimer's disease. *J Comp Neurol* 2013;521:4124–44 [CrossRef Medline](#)
6. Liu AK, Chang RC, Pearce RK, et al. Nucleus basalis of Meynert revisited: anatomy, history and differential involvement in Alzheimer's and Parkinson's disease. *Acta Neuropathol* 2015;129:527–40 [CrossRef Medline](#)
7. Sassini I, Schultz C, Thal DR, et al. Evolution of Alzheimer's disease-related cytoskeletal changes in the basal nucleus of Meynert. *Acta Neuropathol* 2000;100:259–69 [CrossRef Medline](#)
8. Insausti R, Juottonen K, Soininen H, et al. MR volumetric analysis of the human entorhinal, perirhinal, and temporopolar cortices. *AJNR Am J Neuroradiol* 1998;19:659–71 [Medline](#)
9. Teipel SJ, Flatz WH, Heinsen H, et al. Measurement of basal forebrain atrophy in Alzheimer's disease using MRI. *Brain* 2005;128:2626–44 [CrossRef Medline](#)
10. Grothe M, Heinsen H, Teipel SJ. Atrophy of the cholinergic basal forebrain over the adult age range and in early stages of Alzheimer's disease. *Biol Psychiatry* 2012;71:805–13 [CrossRef Medline](#)
11. Grothe MJ, Ewers M, Krause B, et al. Basal forebrain atrophy and cortical amyloid deposition in nondemented elderly subjects. *Alzheimers Dement* 2014;10:S344–53 [CrossRef Medline](#)
12. Förstl H, Levy R, Burns A, et al. Disproportionate loss of noradrenergic and cholinergic neurons as cause of depression in Alzheimer's disease: a hypothesis. *Pharmacopsychiatry* 1994;27:11–15 [CrossRef Medline](#)
13. Bottini G, Berlingeri M, Basilio S, et al. Good or bad responder? Behavioural and neuroanatomical markers of clinical response to donepezil in dementia. *Behav Neurol* 2012;25:61–72 [Medline](#)
14. Hanyu H, Tanaka Y, Sakurai H, et al. Atrophy of the substantia innominata on magnetic resonance imaging and response to donepezil treatment in Alzheimer's disease. *Neurosci Lett* 2002;319:33–36 [CrossRef Medline](#)
15. Kanetaka H, Hanyu H, Hirao K, et al. Prediction of response to donepezil in Alzheimer's disease: combined MRI analysis of the substantia innominata and SPECT measurement of cerebral perfusion. *Nucl Med Commun* 2008;29:568–73 [CrossRef Medline](#)
16. Meng D, Li X, Bauer M, et al. Alzheimer's disease neuroimaging, I: altered nucleus basalis connectivity predicts treatment response in mild cognitive impairment. *Radiology* 2018;289:775–85 [CrossRef Medline](#)
17. Palmqvist S, Mattsson N, Hansson O. Cerebrospinal fluid analysis detects cerebral amyloid- $\beta$  accumulation earlier than positron emission tomography. *Brain* 2016;139:1226–36 [CrossRef Medline](#)
18. Yushkevich P, Piven J, Hazlett H, et al. User-guided 3D active contour segmentation of anatomical structures: significantly improved efficiency and reliability. *Neuroimage* 2006;31:1116–28 [CrossRef Medline](#)
19. Youden WJ. Index for rating diagnostic tests. *Cancer* 1950;3:32–35 [CrossRef](#)
20. Cicchetti D, Sparrow A. Developing criteria for establishing interrater reliability of specific items: applications to assessment of adaptive behavior. *Am J Ment Defic* 1981;86:127–37 [Medline](#)
21. Hanyu H, Asano T, Sakurai F, et al. MR analysis of the substantia innominata in normal aging. *AJNR Am J Neuroradiol* 2002;23:27–32 [Medline](#)
22. Berger-Sweeney J, Heckers S, Mesulam MM, et al. Differential effects on spatial navigation of immunotoxin-induced cholinergic lesions of the medial septal area and nucleus basalis magnocellularis. *J Neurosci* 1994;14:4507–19 [CrossRef Medline](#)
23. George S, Mufson EJ, Leurgans S, et al. MRI-based volumetric measurement of the substantia innominata in amnesic MCI and mild AD. *Neurobiol Aging* 2011;32:1756–64 [CrossRef Medline](#)
24. Dubois B, Feldman HH, Jacova C, et al. Advancing research diagnostic criteria for Alzheimer's disease: the IWG-2 criteria. *Lancet Neurol* 2014;13:614–29 [CrossRef Medline](#)
25. Grothe MJ, Heinsen H, Amaro E, et al. Cognitive correlates of basal forebrain atrophy and associated cortical hypometabolism in mild cognitive impairment. *Cereb Cortex* 2016;26:2411–26 [CrossRef Medline](#)
26. Buerger K, Alafuzoff I, Ewers M, et al. No correlation between CSF tau protein phosphorylated at threonine 181 with neocortical neurofibrillary pathology in Alzheimer's disease. *Brain* 2007;130:E82 [CrossRef Medline](#)
27. Duara R, Loewenstein DA, Potter E, et al. Medial temporal lobe atrophy on MRI scans and the diagnosis of Alzheimer disease. *Neurology* 2008;71:1986–92 [CrossRef Medline](#)
28. Jethwa K, Aphiwatthanasumet K, Mougou O, et al. Phase enhanced PSIR T1-weighted imaging improves contrast resolution of the nucleus basalis of Meynert at 7 T: a preliminary study. *Magn Reson Imaging* 2019;61:296–99 [CrossRef Medline](#)